ELSEVIER

www.elsevier.nl/locate/jorganchem

Journal of Organometallic Chemistry 614–615 (2000) 75–82

Journal of Organo metallic Chemistry

New alkyne bridged mixed-metal clusters and studies of their activity for catalytic hydrosilylation of alkynes

Richard D. Adams *, Uwe Bunz, Burjor Captain, Wei Fu, Winfred Steffen

Department of Chemistry and Biochemistry, University of South Carolina, Columbia, SC 29208, USA

Received 26 January 2000; accepted 25 May 2000

Dedicated to Professor Sheldon G. Shore on the occasion of his 70th birthday.

Abstract

The homologous series of compounds $MPt_2(CO)_5(PPh_3)_2(PhC_2Ph)$, M = Fe (**1**), M = Ru (**3**) and M = Os (**4**) were obtained in the yields 55%, 24% and 30% from the reactions of $Pt(PPh_3)_2(PhC_2Ph)$ with $Fe(CO)_5$, $Ru_3(CO)_{10}$, and $Os(CO)_5$, respectively. Each of the products was characterized by IR, elemental analysis and a single crystal X-ray diffraction analysis. A second mixed-metal cluster product, $Ru_2Pt(CO)_7(PPh_3)_2(PhC_2Ph)$ (**2**) (45% yield) was also obtained from the reaction that yielded **3**. In fact, it is obtained in a higher yield than that of **3**. Compounds **1**, **3**, and **4** are isostructural and are comprised of a MPt_2 (M = Fe, Ru or Os) triangular metal cluster containing a triply bridging diphenylacetylene ligand. The structure of compound **2** is similar to that of **1**, **3**, and **4**, but contains two ruthenium and one platinum atom in the triangular cluster. One coproduct $Os(CO)_2(PPh_3)_2(PhC_2Ph)$ (**5**) (25% yield) was obtained from the reaction of $Os(CO)_5$ with $Pt(PPh_3)_2(PhC_2Ph)$. Compound **5** contains only one metal atom with an approximately trigonal bipyramidal coordination having the two phosphine ligands in the axial positions and the alkyne in an equatorial site. The reaction of **2** with H_2 in refluxing hexane afforded the tetranuclear complex $H_2Ru_2Pt_2(CO)_8(PPh_3)_2$ (**6**) (11% yield) that contains an Ru_2Pt_2 tetrahedral shaped cluster with two bridging hydride ligands. The ability of the solutions of compounds **1**–**6** and $Pt(PPh_3)_2(PhC_2Ph)$ to produce catalytic hydrosilylation of diphenylacetylene by triethylsilane to yield (*E*)-[(1,2-diphenyl)ethenyl]triethylsilane at 30°C, and 1,4-bis(trimethylsilyl)butadiyne with triethylsilane to yield (*E*)-2-triethylsilyl-1,4-bis(trimethylsilyl)-1-buten-3-yne at 60°C was investigated. $Pt(PPh_3)_2(PhC_2Ph)$ was the best catalyst for these reactions. Compound **5** is completely inactive. A combination of evidence suggests that the catalytic activity exhibited by the mixed-metal cluster complexes is produced principally by fragmentation products which are almost certainly mononuclear platinum complexes. © 2000 Elsevier Science B.V. All rights reserved.

Keywords: Platinum; Ruthenium; Alkyne; Cluster; Hydrosilylation; Catalysis

1. Introduction

Mixed-metal heterogeneous catalysts have attracted much interest because their catalytic properties are often superior to that of their components [1]. Various mechanisms of cooperativity have been proposed. For example, it has been suggested that a metal atom can activate its neighbor simply through the donation of electron density [2]. It has also been proposed that the different metals may exhibit bifunctional cooperativity such that one metal performs one role in a catalytic reaction and the other performs a second function [3]. Metal cluster complexes have been considered as fragments of a metal surface surrounded by a layer of 'adsorbed' ligand molecules [4], and the 'cluster/surface' analogy was proposed in the late 1970s to show the connections between cluster chemistry to heterogeneous catalysis [5].

We have recently reported that the layer segregated platinum/ruthenium cluster complex $Pt_3Ru_6(CO)_{20}(\mu_3\text{-}PhC_2Ph)H_2$ exhibits good catalytic activity for the hydrosilylation of alkynes under homogeneous conditions [6], however a study of the catalytic hydrosilylation of alkenes by $Ru_3(CO)_{12}$ has indicated cluster fragmentation processes are important in this case [7].

Here we report the synthesis and characterization of the new heteronuclear three metal cluster complexes $MPt_2(CO)_5(PPh_3)_2(PhC_2Ph)$ where M = Fe (**1**), Ru (**3**),

---

* Corresponding author. Tel.: + 1-803-777-7187; fax: + 1-803-777-6781.

E-mail address: adams@psc.sc.edu (R.D. Adams).

PII: S0022-328X(00)00302-8

Os (**4**) that were obtained from the reactions of $Pt(PPh_3)_2(PhC_2Ph)$ with $Fe(CO)_5$, $Ru_3(CO)_{12}$ and $Os(CO)_5$, respectively. Coproducts $Ru_2Pt(CO)_7(PPh_3)(PhC_2Ph)$ (**2**) and $Os(CO)_2(PPh_3)_2(PhC_2Ph)$ (**5**) that were also obtained from the ruthenium and osmium reactions were fully characterized. In addition, the reaction of compound **2** with H_2 in a refluxing hexane solution yielded the new tetranuclear cluster complex $H_2Ru_2Pt_2(CO)_8(PPh_3)_2$ (**6**). The ability of compounds **1**–**6** and the mononuclear complex $Pt(PPh_3)_2(PhC_2Ph)$ to produce catalytic hydrosilylation of diphenylacetylene by triethylsilane to yield (*E*)-[(1,2-diphenyl)-ethenyl]triethylsilane, and 1,4-bis(trimethylsilyl)-butadiyne with triethylsilane to yield (*E*)-2-triethylsilyl-1,4-bis(trimethylsilyl)-1-buten-3-yne were also investigated and are reported here. The evidence indicates that fragmentation processes are probably important and may involve mononuclear platinum complexes as the true catalysts.

2. Experimental

2.1. General data

All reactions were performed under a nitrogen atmosphere. Reagent grade solvents were dried by the standard procedures and were freshly distilled prior to use. Infrared spectra were recorded on a Nicolet 5DXBO FTIR spectrophotometer. ^1H-NMR and ^{31}P-NMR were recorded on a Varian Inova 400 spectrometer operating at 399.9 and 161.9 MHz, respectively. Elemental analyses were performed by Oneida Research Services (Whitesboro, NY, USA) and Desert Analytics (Tucson, AZ, USA). $Fe(CO)_5$ and $Ru_3(CO)_{12}$ were purchased from Aldrich and Strem, respectively, and were used without further purification. $Pt(PPh_3)_2(PhC_2Ph)$[8] and $Os(CO)_5$[9] were prepared according to the published procedures. Product separations were performed by TLC in air on Analtech 0.25 and 0.5 mm silica gel 60 Å F_{254} glass plates.

2.2. Reaction of $Fe(CO)_5$ with $Pt(PPh_3)_2(PhC_2Ph)$

A 67.0-mg amount of $Pt(PPh_3)_2(PhC_2Ph)$ (0.074 mmol) was dissolved in 10 ml of toluene in a 25 ml three-neck round-bottom flask. A 12.7-μl amount of $Fe(CO)_5$ (0.097 mmol) were added via syringe, and the reaction mixture was then heated to reflux for 45 min. After cooling, the solvent was then removed in vacuo, and the product was purified by TLC using a 1:1 hexane–methylene chloride solvent mixture to yield 53.0 mg (55%) of an orange product, $FePt_2(CO)_5(PPh_3)_2(PhC_2Ph)$ (**1**). Spectral data for **1**: IR ν_{CO} (cm^{-1} in CH_2Cl_2): 2041 (s), 2012 (m, sh), 1989 (s), 1930 (m, br). Anal. Calc.: C, 51.25; H, 3.13. Found: C, 51.51; H, 3.18%.

2.3. Reaction of $Ru_3(CO)_{12}$ with $Pt(PPh_3)_2(PhC_2Ph)$

A 105.0-mg amount of $Ru_3(CO)_{12}$ (0.165 mmol) and 150.0 mg of $Pt(PPh_3)_2(PhC_2Ph)$ (0.167 mmol) were dissolved in 15 ml of toluene in a 25 ml three-neck round-bottom flask equipped with a stir bar at 25°C. Immediately, the color of the solution turned dark red. The reaction mixture was then heated to reflux for 30 min. After cooling, the solvent was removed in vacuo, and the products were separated by TLC using a 3:1 hexane–methylene chloride solvent mixture. The compounds eluted in the following order were: $Ru_3(CO)_{12}$ (yellow, trace); $Ru_4(CO)_{12}(PhC_2Ph)$ [10] (brown, 1.8 mg, 1%); $Ru_3(CO)_{11}(PPh_3)$ [11] (orange, 30.2 mg, 21%); $Ru_3(CO)_7(PPh_2)_2(\mu\text{-}C_6H_5)$ [12] (red, trace); $Ru_3(CO)_8(\mu\text{-}C_4Ph_4)$ [13] (orange–yellow, trace); $Ru_2Pt(CO)_7(PPh_3)_2(PhC_2Ph)$ (dark red–brown, 76.8 mg, 45%) (**2**); $Ru_3(CO)_{10}(PPh_3)_2$ [14] (red, 7.0 mg, 4%); $RuPt_2(CO)_5(PPh_3)_2(PhC_2Ph)$ (orange–yellow, 53.0 mg, 24%) (**3**). Spectral data for **2**: IR ν_{CO} (cm^{-1} in hexane): 2068 (s), 2034 (m, sh), 2029 (vs), 1992 (m), 1980 (m), 1964 (m). Anal. Calc.: C, 42.94; H, 2.43. Found: C, 42.60; H, 2.44%. Spectral data for **3**: IR ν_{CO} (cm^{-1} in CH_2Cl_2): 2045 (s), 2011 (s), 1961 (m). ^{31}P-NMR (d_8-toluene): $\delta = 17.64$ ppm; $^1J_{P-Pt} = 3417$ Hz; $^2J_{P-Pt} = 168$ Hz. Anal. Calc.: C, 49.47; H, 3.00. Found: C, 49.56; H, 3.00%.

2.4. Reaction of $Os(CO)_5$ with $Pt(PPh_3)_2(PhC_2Ph)$

A 80.0-mg amount of $Pt(PPh_3)_2(PhC_2Ph)$ (0.089 mmol) dissolved in 5 ml of toluene was added to a 50 ml three-neck round-bottom flask containing a 30 ml solution of $Os(CO)_5$ in hexane (ca. 2 mg ml^{-1}). The reaction mixture was heated to reflux and stirred for 1 h, after which the volatiles were removed in vacuo. The products were separated by TLC using a 3:1 hexane–methylene chloride solvent mixture to yield 21.0 mg (25%) of $Os(CO)_2(PPh_3)_2(PhC_2Ph)$ (**5**), and 38.5 mg (30%) of $OsPt_2(CO)_5(PPh_3)_2(PhC_2Ph)$ (**4**). Spectral data for **4**: IR ν_{CO} (cm^{-1} in CH_2Cl_2): 2047 (s), 2011 (s), 1952 (m). Anal. Calc.: C, 46.41; H, 2.83. Found: C, 46.07; H, 2.63%. Spectral data for **5**: IR ν_{CO} (cm^{-1} in CH_2Cl_2): 1958 (s), 1892 (vs). Anal. Calc.: C, 65.81; H, 4.24. Found: C, 65.41; H, 3.84%.

2.5. Reaction of **2** with H_2

A 42.0-mg amount of **2** was dissolved in 40 ml of hexane in a 100 ml three-neck round-bottom flask equipped with a stir bar, reflux condenser, and gas inlet. The solution was then heated to reflux and purged with hydrogen (1 atm) for 1 h. After the solvent was removed the reaction mixture was transferred to TLC plates and separated by using a 3:1 hexane–methylene chloride solvent mixture to yield 6.0 mg of

$H_4Ru_4(CO)_{11}(PPh_3)$ [15,16] (18% yield) and 5.6 mg of $H_2Ru_2Pt_2(CO)_8(PPh_3)_2$ (**6**) (11% yield). Spectral data for **6**: IR ν_{CO} (cm^{-1} in hexane): 2082 (w), 2060 (s), 2032 (vs) 2009 (m, sh), 1989 (s), 1957 (m). ^{1}H-NMR ($CDCl_3$ in ppm): $\delta = 7.22–7.40$ (m, 30H, Ph), $\delta = -8.21$ (d, 2H, μ-H, $^2J_{P-H} = 21$ Hz, $^1J_{Pt-H} = 289$ Hz). Anal. Calc.: C, 39.35; H, 2.40. Found: C, 40.61; H, 2.74%.

2.6. Crystallographic analysis

Orange crystals of **1**, dark red–brown crystals of **2**, orange–yellow crystals of **3**, yellow crystals of **4** and **5**, and dark red crystals of **6** suitable for diffraction analysis were grown by slow evaporation of solvent from solutions in hexane–methylene chloride solvent mixtures at 25°C. All crystals used for the diffraction measurements were mounted in thin-walled glass capillaries. Diffraction measurements were made on a Rigaku AFC6S fully automated four-circle diffractometer using graphite-monochromated Mo–K_α radiation. The unit cells of the crystals were determined and refined from 15 randomly selected reflections obtained by using the AFC6 automatic search, center, index, and least squares routines. All data processing was performed on a Silicon-Graphics INDIGO [2] workstation by using the TEXSAN structure solving program library obtained from the Molecular Structure, The Woodlands, TX, USA. Neutral atom scattering factors were calculated by the standard procedures [17]. Anomalous dispersion corrections were applied to all non-hydrogen atoms [18]. Lorentz/polarization (Lp) corrections were applied to the data for each structure. Full-matrix least-squares refinements minimized the function: $\Sigma_{hkl} w(|F_o| - |F_c|)^2$, where $w = 1/\sigma^2(F)$, $\sigma(F) = \sigma(F_o^2)/2F_o$ and $\sigma(F_o^2) = [\sigma(I_{raw})^2 + (0.08I_{net})^2]^{1/2}/Lp$.

Compounds **1**, **3**, and **4** are isomorphous and crystallized in the orthorhombic crystal system. The space group *Pbca* was established on the basis of the systematic absences observed during the collection of the intensity data. The structures were solved by a combination of direct methods (SIR92) and difference Fourier syntheses. For compound **1**, all non-hydrogen atoms in the structures were refined with anisotropic thermal parameters. For compounds **3** and **4**, all atoms in the structure except for the carbon atoms on the triphenylphosphine ligand and the hydrogen atoms, were refined with anisotropic thermal parameters. Each compound crystallized with one equivalent of hexane in the crystal lattice. It was located and refined in the analyses of **1** and **3**. In **4** it was located, partially refined and then fixed on the final cycles because it would not refine to convergence. For all three structural analyses, the hydrogen atoms were calculated and included as fixed contributions to the scattering.

Compound **2** crystallized in the monoclinic crystal system. The space group $P2_1/c$ was identified uniquely on the basis of systematic absences observed during the collection of the intensity data. The structure was solved by a combination of direct methods (SIR92) and difference Fourier syntheses. All non-hydrogen atoms were refined with anisotropic thermal parameters. In the final stages of the analysis, one equivalent of methylene chloride from the crystallization solvent was found co-crystallized in the crystal lattice. This molecule was included in the crystal structure analysis and was refined satisfactorily.

Compound **5** crystallized in the triclinic crystal system. The space group $P\bar{1}$ was assumed and confirmed by the successful solution and refinement of the structure. The structure was solved by a combination of direct methods (SIR92) and difference Fourier syntheses. All non-hydrogen atoms were refined with anisotropic thermal parameters.

Compound **6** crystallized in the monoclinic crystal system. The space group $P2_1/c$ was identified uniquely on the basis of the systematic absences observed during the collection of the intensity data. The structure was solved by a combination of direct methods (SIR92) and difference fourier syntheses. All non-hydrogen atoms were refined with anisotropic thermal parameters. The two hydride ligands were located and refined. In the final stages of the analysis, one equivalent of hexane from the crystallization solvent was found co-crystallized in the crystal lattice. The molecule was included in the crystal structure analysis and was refined satisfactorily. Crystallographic data for compounds **1**–**6** are listed in Tables 1 and 2.

2.7. General procedures for the catalysis studies

All reactions were performed under a nitrogen atmosphere. Diphenylacetylene, triethylsilane, and d_8-toluene were purchased from Aldrich and were used without further purification. 1,4-bis(trimethylsilyl)butadiyne was purchased from Aldrich and was recrystallized using hexane prior to use. $CDCl_3$ solvent was purchased from Cambridge Isotope Laboratories and used as received. C_6Me_6 purchased from Aldrich was used as an internal calibration for determining the amounts of product for the hydrosilylation of diphenylacetylene reaction. Turnover frequencies (TOF) were obtained by measuring the product formed by ^{1}H-NMR spectroscopy.

2.8. Catalytic hydrosilations of diphenylacetylene

In a typical run a 2.9-mg amount of **1** (0.00225 mmol), 40-mg amount of PhC_2Ph (0.225 mmol), and 10-mg amount of C_6Me_6 was all dissolved in 1.5 ml of $CDCl_3$ in a 5 ml round-bottom flask equipped with a stir bar. The solution was stirred to ensure that all of the complex had dissolved completely. Two portions of 0.6 ml of this solution were then transferred via syringe to two clean sealed 5 mm NMR tubes. To each of these tubes 144 µl of Et_3SiH (0.9 mmol, 1000 equivalents to **1**) was added. The NMR tubes were then evacuated and filled with nitrogen three times, after which they were placed in an oil bath maintained at a temperature of 30°C for 1 h. ^{1}H-NMR spectra of the reaction mixture showed that 2.0% of PhC_2Ph was converted to (*E*)-[(1,2-diphenyl)ethenyl]triethylsilane [19]. Similarly

Table 1
Crystallographic data for diffraction studies

Compound	**1**	**3**	**4**
Empirical formula	$Pt_2FeP_2O_5C_{55}H_{40} \cdot C_6H_{14}$	$Pt_2RuP_2O_5C_{55}H_{40} \cdot C_6H_{14}$	$Pt_2OsP_2O_5C_{55}H_{40} \cdot C_6H_{14}$
Formula weight	1375.07	1420.29	1509.42
Crystal system	Orthorhombic	Orthorhombic	Orthorhombic
Lattice parameters			
a (Å)	21.407(2)	21.422(3)	21.408(6)
b (Å)	19.973(7)	19.839(3)	19.848(5)
c (Å)	24.029(4)	24.115(5)	24.135(9)
V (Å^3)	10 274(35)	10 248(2)	10 255(4)
Space group	*Pbca* (no. 61)	*Pbca* (no. 61)	*Pbca* (no. 61)
Z value	8	8	8
ρ_{calc} (g cm^{-3})	1.78	1.84	1.96
μ (Mo–K$_\alpha$) (cm^{-1})	58.0	58.3	80.0
Temperature (°C)	20	20	20
$2\Theta_{max}$ (°)	40.0	42.0	40.0
No. of observations ($I > 3\sigma(I)$)	3124	3464	3385
No. of variables	576	431	406
Goodness-of-fit (GoF) [a]	1.32	1.56	1.21
Max. shift in cycle	0.04	0.02	0.00
Residuals: R, R_w	0.050, 0.064	0.047, 0.052	0.042, 0.060
Absorption correction	DIFABS	DIFABS	DIFABS
Transmissions coefficient, max/min	1.00/0.55	1.00/0.83	1.00/0.42
Largest peak in final difference map (e Å^{-3})	1.03	1.42	1.51

[a] $R = \Sigma_{hkl}(|F_{obs}| - |F_{calc}||)/\Sigma_{hkl}|F_{obs}|$; $R_w = [\Sigma_{hkl}\, w(|F_{obs}| - |F_{calc}|)^2/\Sigma_{hkl}\, wF^2_{obs}]^{1/2}$, $w = 1/\sigma^2(F_{obs})$; GoF $= [\Sigma_{hkl}\, w(|F_{obs}| - |F_{calc}|)^2/(n_{data} - n_{vari})]^{1/2}$.

Table 2
Crystallographic data for diffraction studies

Compound	**2**	**5**	**6**
Empirical formula	$PtRu_2PO_7C_{39}H_{25} \cdot CH_2Cl_2$	$OsP_2O_2C_{52}H_{40}$	$Pt_2Ru_2P_2O_8C_{44}H_{32} \cdot C_6H_{14}$
Formula weight	1118.76	949.03	1343.00
Crystal system	Monoclinic	Triclinic	Monoclinic
Lattice parameters			
a (Å)	12.813(2)	12.298(4)	11.156(1)
b (Å)	19.791(3)	15.627(4)	16.345(4)
c (Å)	17.022(6)	11.205(2)	28.577(5)
α (°)	90	98.41(2)	90
β (°)	110.96(1)	92.49(2)	99.11(1)
γ (°)	90	77.34(2)	90
V (Å^3)	4031(2)	2078(1)	5145(1)
Space group	$P2_1/c$ (no. 14)	$P\bar{1}$ (no. 2)	$P2_1/c$ (no. 14)
Z value	4	2	4
ρ_{calc} (g cm^{-3})	1.84	1.52	1.73
μ (Mo–K$_\alpha$) (cm^{-1})	44.1	31.8	60.9
No. of obsevations ($I > 3\sigma(I)$)	3493	3653	3627
No. of variables	479	514	531
Goodness-of-fit (GoF) [a]	1.25	1.00	1.03
Max. shift in cycle	0.00	0.00	0.02
Residuals*: R, R_w	0.026, 0.029	0.029, 0.035	0.030, 0.040
Absorption correction	DIFABS	DIFABS	DIFABS
Transmission coefficient, max/min	1.00/0.66	1.00/0.76	1.00/0.65
Largest peak in final difference map (e Å^{-3})	0.52	0.50	0.54

[a] $R = \Sigma_{hkl}(||F_{obs}| - |F_{calc}||)/\Sigma_{hkl}|F_{obs}|$; $R_w = [\Sigma_{hkl}\, w(|F_{obs}| - |F_{calc}|)^2/\Sigma_{hkl}\, wF^2_{obs}]^{1/2}$, $w = 1/\sigma^2(F_{obs})$; GoF $= [\Sigma_{hkl}\, w(|F_{obs}| - |F_{calc}|)^2/(n_{data} - n_{vari})]^{1/2}$.

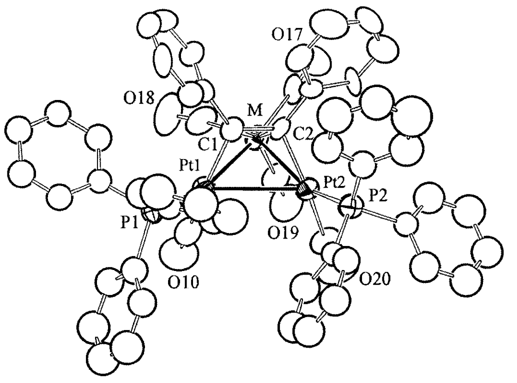

Fig. 1. An ORTEP diagram representing the molecular structures of compounds **1**, **3**, and **4** (M = Fe, Ru and Os).

3.0 mg of **3** (0.00225 mmol) converted 16.1% of PhC_2Ph to (*E*)-[(1,2-diphenyl)ethenyl]triethylsilane, and 3.2 mg of **4** (0.00225 mmol) converted 8.0% of PhC_2Ph to (*E*)-[(1,2-diphenyl)ethenyl]triethylsilane under the same conditions. The catalysis of compounds **2**, **5**, **6** and $Pt(PPh_3)_2(PhC_2Ph)$ were conducted similarly.

2.9. Catalytic hydrosilations of 1,4-bis(trimethylsilyl)butadiyne

2.9.1. Determination of initial rates

A 2.8-mg amount of **1** (0.00217 mmol) and a 42.0-mg amount of 1,4-bis(trimethylsilyl)butadiyne (0.217 mmol) were all dissolved in 0.60 ml of d_8-toluene in a 5-ml round-bottom flask equipped with a stir bar. The solution was stirred until all of the **1** had dissolved completely. Then, a 69-µl amount of Et_3SiH (0.433 mmol) was added via syringe. The reaction flask was then partially evacuated and filled with nitrogen three times. It was then placed in a constant temperature oil bath at a temperature of 60°C for 1 h. ^{1}H-NMR of the reaction mixture showed that 4.7% of 1,4-bis(trimethylsilyl)butadiyne was converted to (*E*)-2-triethylsilyl-1,4-bis(trimethylsilyl)-1-buten-3-yne [20]. Similarly, 2.9 mg of **3** (0.00217 mmol) converted 16% of 1,4-bis(trimethylsilyl)butadiyne to (*E*)-2-triethylsilyl-1,4-bis(trimethylsilyl)-1-buten-3-yne, and 3.1 mg of **4** (0.00217 mmol) converted 13% of 1,4-bis(trimethylsilyl)butadiyne to (*E*)-2-triethylsilyl-1,4-bis(trimethylsilyl)-1-buten-3-yne under the same conditions. The catalysis of compounds **2**, **5**, **6** and $Pt(PPh_3)_2(PhC_2Ph)$ were conducted similarly.

2.9.2. Long term

In a similar manner, a 2.8-mg amount of **1** (0.00217 mmol) and a 211-mg amount of 1,4-bis(trimethylsilyl)butadiyne (1.09 mmol) was all dissolved in 0.8 ml of d_8-toluene in a 5-ml round-bottom flask equipped with a reflux condensor and a stir bar. The solution was stirred until all of the **1** had dissolved completely. Then, a 347-µl amount of Et_3SiH (2.17 mmol) was then added to the reaction flask. The reaction flask was then evacuated and filled with nitrogen three times. The flask was then placed in an oil bath maintained at a temperature of 60°C for 7 h. A ^{1}H-NMR spectrum of the reaction mixture showed that 100% of 1,4-bis(trimethylsilyl)butadiyne was converted to (*E*)-2-triethylsilyl-1,4-bis(trimethylsilyl)-1-buten-3-yne [20]. Similarly 2.9 mg of **3** (0.00217 mmol) converted 100% of 1,4-bis(trimethylsilyl)butadiyne to (*E*)-2-triethylsilyl-1,4-bis(trimethylsilyl)-1-buten-3-yne, and 3.1 mg of **4** (0.00217 mmol) converted 100% of 1,4-bis(trimethylsilyl)butadiyne to (*E*)-2-triethylsilyl-1,4-bis(trimethylsilyl)-1-buten-3-yne under the same conditions.

3. Results and discussion

The homologous series of compounds $MPt_2(CO)_5(PPh_3)_2(PhC_2Ph)$, **1**, M = Fe; **3**, M = Ru and **4**, M = Os were obtained in the yields 55%, 24% and 30% from the reactions of $Pt(PPh_3)_2(PhC_2Ph)$ with $Fe(CO)_5$, $Ru_3(CO)_{12}$, and $Os(CO)_5$, respectively. Each of the products was characterized by IR, elemental and a single crystal X-ray diffraction analysis. All three compounds are isostructural and isomorphous. An ORTEP diagram representing the molecular structure of these compounds is shown in Fig. 1. A listing of selected interatomic distances and angles are given in Table 3. Each compound consists of a triangular Pt_2M cluster with a triply bridging diphenylacetylene ligand. In each case the Pt–Pt distance is long, Pt–Pt = 3.013(1) Å for **1**, 3.066(1) Å for **3**, and 3.080(1) Å for **4** and can be regarded as a very weak bond or no bond at all. The alkyne C–C bond is parallel to the Pt–Pt bond and the C–C distance C(1)–C(2): 1.30(3) Å for **1**, 1.42(2) Å for **3** and 1.39(2) Å for **4**, is slightly longer than that found for the uncoordinated alkyne, 1.20 Å, as expected due to the effects of its coordination. The molecular structure of these compounds is very similar to that of the related compounds $Pt_2M(\mu_3\text{-}\eta^1{:}\eta^1{:}\eta^2\text{-}PhC{\equiv}CC{\equiv}CPh)(CO)_5(PPh_3)_2$, M = Fe, **7** [21] and Ru, **8** [21] which were recently reported and also exhibit a long Pt–Pt distance, 2.939(2) and 3.072(1) Å for the two different crystalline forms of **7**. Each platinum atom coordinated with one triphenylphosphine ligand and one carbonyl ligand while the heterometal atom is coordinated with three carbonyl ligands. Assuming that the alkyne serves as a four-electron donor, each cluster contains a total of 46 electrons which is two electrons less than the 48 electrons expected for a triangular cluster where all three metal atoms obey the 18-electron rule. Previous studies have shown that clusters containing diplatinum groups often contain fewer electrons than that predicted by the conventional electron counting theories [22].

Table 3
Selected intramolecular bond distances and angles for **1**, **3** and **4**

Compound **1**		Compound **3**		Compound **4**	
Atom–atom	Distance	Atom–atom	Distance	Atom–atom	Distance
Intramolecular bond distances [a]					
Pt(1)–Pt(2)	3.013(1)	Pt(1)–Pt(2)	3.066(1)	Pt(1)–Pt(2)	3.080(1)
Pt(1)–Fe	2.531(3)	Pt(1)–Ru	2.623(2)	Pt(1)–Os	2.647(1)
Pt(1)–P(1)	2.326(6)	Pt(1)–P(1)	2.325(5)	Pt(1)–P(1)	2.317(5)
Pt(1)–C(1)	2.09(2)	Pt(1)–C(1)	2.04(2)	Pt(1)–C(1)	2.09(2)
Pt(2)–Fe	2.608(3)	Pt(2)–Ru	2.676(2)	Pt(2)–Os	2.688(1)
Pt(2)–P(2)	2.319(6)	Pt(2)–P(2)	2.291(5)	Pt(2)–P(2)	2.315(6)
Pt(2)–C(2)	2.11(2)	Pt(2)–C(2)	2.04(2)	Pt(2)–C(2)	2.10(2)
Fe–C(1)	2.14(2)	Ru–C(1)	2.25(2)	Os–C(1)	2.26(2)
Fe–C(2)	2.14(2)	Ru–C(2)	2.29(2)	Os–C(2)	2.29(2)
C(1)–C(2)	1.30(3)	C(1)–C(2)	1.42(2)	C(1)–C(2)	1.39(2)
Atom–atom–atom	Angle	Atom–atom–atom	Angle	Atom–atom–atom	Angle
Intramolecular bond angles [b]					
Pt(2)–Pt(1)–Fe	55.30(7)	Pt(2)–Pt(1)–Ru	55.46(4)	Pt(2)–Pt(1)–Os	55.37(3)
Pt(1)–Pt(2)–Fe	52.91(7)	Pt(1)–Pt(2)–Ru–	55.83(4)	Pt(1)–Pt(2)–Os	54.12(3)
Pt(1)–Fe–Pt(2)	71.79(8)	Pt(1)–Ru–Pt(2)	70.71(4)	Pt(1)–Os–Pt(2)	70.51(3)

[a] Distances are in Å. Estimated S.D.s in the least significant figure are given in parentheses.

[b] Angles are in degrees (°). Estimated S.D.s in the least significant figure are given in parentheses.

A second mixed-metal cluster product, $Ru_2Pt(CO)_7(PPh_3)_2(PhC_2Ph)$ (**2**) (45%) was also obtained from the reaction that yielded **3**. In fact, it is obtained in a higher yield than that of **3**. Compound **2** was also characterized crystallographically, and an ORTEP diagram of its structure is shown in Fig. 2. Compound **2** contains a triangular cluster composed of one platinum and two ruthenium atoms. The diphenylacetylene ligand is coordinated as a triply bridging ligand as in **3**, but the C–C bond of the alkyne is parallel to one of the Ru–Pt bonds. Each ruthenium atom has three carbonyl ligands while the platinum atom contains the triphenylphosphine and one carbonyl ligand. All metal atoms have 18-electron configurations and a no unusual metal–metal bond distances.

One coproduct $Os(CO)_2(PPh_3)_2(PhC_2Ph)$ (**5**) (25% yield) was obtained from the reaction of $Os(CO)_5$ with $Pt(PPh_3)_2(PhC_2Ph)$. Compound **5** was also characterized by IR, elemental and single crystal X-ray diffraction analyses. An ORTEP diagram of the molecular structure of **5** is shown in Fig. 3. Compound **5** contains only one metal atom. The C–C bond distance of the diphenylacetylene ligand in **5** is 1.31(1) Å. The coordination geometry of the osmium atom is approximately trigonal bipyramidal with the two phosphine ligands in the axial positions. The diphenylacetylene ligand serves as a two electron donor and the osmium atom has an 18-electron configuration.

When a hexane solution of compound **2** was heated to reflux in the presence of a slow purge with H_2, the new tetranuclear mixed metal cluster compound $Ru_2Pt_2(CO)_8(PPh_3)_2(\mu\text{-}H)_2$ (**6**) was formed in 11% yield. Compound **6** was characterized by IR, elemental and single crystal X-ray diffraction analyses, and an ORTEP diagram of its molecular structure is shown in Fig. 4. The molecule contains two ruthenium atoms and two platinum atoms in a tetrahedral arrangement. The two hydride ligands bridge two of the Ru–Pt bonds. The electron count for the cluster is 58 which is two less than the expected 60 electron count. However, it has been found that platinum containing tetrahedral clusters often contain 58 electrons [22].

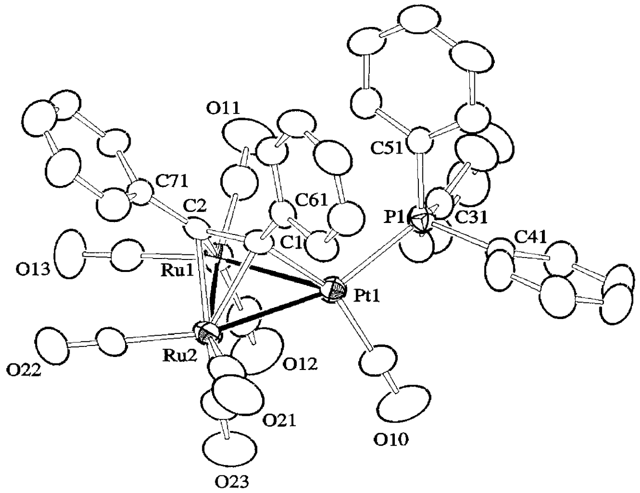

Fig. 2. An ORTEP diagram of $Ru_2Pt(CO)_7(PPh_3)_2(PhC_2Ph)$ (**2**). Selected bond distances (Å) for **2**. Pt(1)–Ru(1) 2.7935(6), Pt(1)–Ru(2) 2.6584(6), Ru(1)–Ru(2) 2.6887(9), Pt(1)–C(1) 2.051(7), Ru(1)–C(2) 2.060(7), Ru(2)–C(1) 2.230(6), Ru(2)–C(2) 2.260(7), Pt(1)–P(1) 2.338(2), Pt(1)–C(10) 1.90(1), Ru(1)–C(av) 1.910(7), Ru(2)–C(av) 1.88(2), C(1)–C(2) 1.391(9).

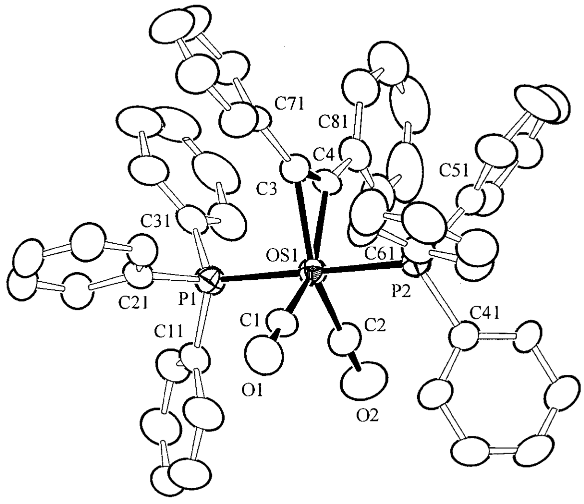

Fig. 3. An ORTEP diagram of $Os(CO)_2(PPh_3)_2(PhC_2Ph)$ (**5**). Selected bond distances (Å) and angles (°) for **5**. Os(1)–P(1) 2.384(2), Os(1)–P(2) 2.400(2), Os(1)–C(1) 1.899(8), Os(1)–C(2) 1.903(9), Os(1)–C(3) 2.169(7), Os(1)–C(4) 2.144(7), C(3)–C(4) 1.31(1), C(1)–Os(1)–C(2) 98.0(3), C(3)–Os(1)–C(4) 35.3(3).

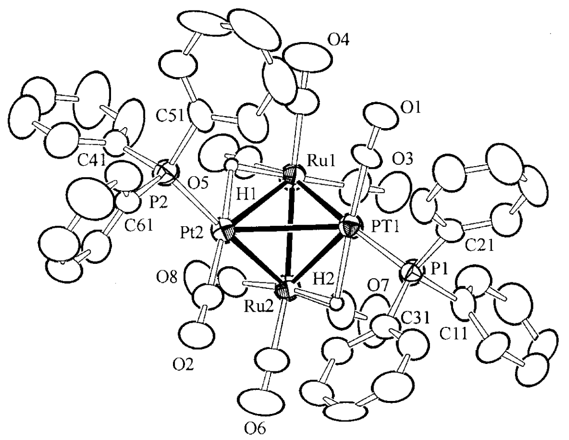

Fig. 4. An ORTEP diagram of $Ru_2Pt_2(CO)_8(PPh_3)_2(\mu\text{-}H)_2$ (**6**). Selected bond distances (Å): Pt(1)–Pt(2) 3.137(1), Pt(1)–Ru(1) 2.711(1), Pt(1)–Ru(2) 2.829(1), Pt(2)–Ru(1) 2.846(1), Pt(2)–Ru(2) 2.732(1), Ru(1)–Ru(2) 2.745(1), Pt(1)–P(1) 2.322(3), Pt(2)–P(2) 2.343(3), Pt(1)–H(2) 2.02, Pt(2)–H(1) 1.81, Ru(1)–H(1) 1.86, Ru(2)–H(2) 1.76.

3.1. Studies of hydrosilation catalysis of alkynes

Ojima [23] and Adams [6] have shown that certain mixed metal complexes can be effective catalysts for the hydrosilylation of alkynes. Accordingly, we have investigated the ability of compounds **1**–**6** and $Pt(PPh_3)_2(PhC_2Ph)$ to serve as catalyst precursors for the hydrosilylation of diphenylacetylene and 1,4-bis(trimethylsilyl)butadiyne with triethylsilane (Eqs. (1) and (2)). Results of our investigations of these catalytic reactions are listed in Tables 4 and 5.

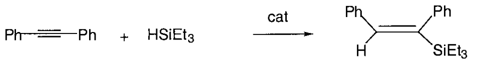

(1)

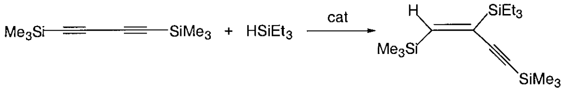

(2)

Solutions of compounds of **1**–**4**, **6** and $Pt(PPh_3)_2(PhC_2Ph)$ were found to be catalytically active. Compound **5** was inactive. The reactions were characterized by 'initial rate' measurements by terminating the reactions at the end of 1 h of reaction time. Except for the reactions of **2**, the solutions **1**, **3**, and **4** after catalysis showed large amounts of the starting cluster complex were still present ($>75\%$ by TLC separations), but trace amounts of other metallic species were also observed. Compound **2** and **6** were the best catalyst precursors, but both also underwent greatest decomposition during catalysis. The catalysis by compounds **1**, **3**, and **4** was further characterized by measuring for a period of 7 h. After 7 h, all of the reactions were complete (100% yield).

Significantly, in the case of the hydrosilylation of 1,4-bis(trimethylsilyl)butadiyne by **1**, **3**, and **4**, the compounds **1**, **3**, and **4** were recovered unchanged, and there was no evidence for the formation of butadiyne complexes, such as **7** and **8**, from the reactions involving **1** and **3**. The absence of any observable replacement of the PhC_2Ph by the 1,4-bis(trimethylsilyl)butadiyne in the catalyses by **1** and **3** was an indication that the diyne was not involved with the intact cluster complexes. Efforts to measure the rates of catalysis as a function of the concentration of the cluster gave poor reproducibility, and it was suspected that cluster fragmentation was occurring and was possibly responsible for the catalysis. Accordingly, the catalytic activity of the two mononuclear complexes **5** and

Table 4
Results for the hydrosilylation of diphenylacetylene and 1,4-bis(trimethylsilyl)butadiyne by **1**, **3**, and **4**

Catalyst	**1** TOF (h^{-1}) at 30°C [a]	**2** TOF (h^{-1}) at 60°C [b]
$FePt_2(CO)_5(PPh_3)_2(PhC_2Ph)$	2.0	4.7
$RuPt_2(CO)_5(PPh_3)_2(PhC_2Ph)$	16	16
$OsPt_2(CO)_5(PPh_3)_2(PhC_2Ph)$	8.0	13
$Ru_2Pt(CO)_7(PPh_3)(PhC_2Ph)$	18	45
$Ru_2Pt_2(CO)_8(PPh_3)_2H_2$	24	15
$Os(CO)_2(PPh_3)_2(PhC_2Ph)$	0	0
$Pt(PPh_3)_2(PhC_2Ph)$	58	100

[a] Catalyst/alkyne/triethylsilane ratio 1/100/1000 for Eq. (1).

[b] Catalyst/diyne/triethylsilane ratio 1/100/200 for Eq. (2).

Table 5
Results of the long term kinetic runs for the hydrosilylation of 1,4-bis(trimethylsilyl)butadiyne by **1**, **3**, and **4**

Catalyst	1,4-bis(trimethylsilyl)butadiyne	Et_3SiH	Time (h)	% Yield
$FePt_2(CO)_5(PPh_3)_2(PhC_2Ph)$	500 equivalents	1000 equivalents	7	100
$RuPt_2(CO)_5(PPh_3)_2(PhC_2Ph)$	500 equivalents	1000 equivalents	7	100
$OsPt_2(CO)_5(PPh_3)_2(PhC_2Ph)$	500 equivalents	1000 equivalents	7	100

$Pt(PPh_3)_2(PhC_2Ph)$ was investigated. Complex **5** was inactive for both hydrosilylation reactions, however $Pt(PPh_3)_2(PhC_2Ph)$ was not only active for both reactions, it was by far the best catalyst of all of those studied, and was even better for the 1,4-bis(trimethylsilyl)butadiyne than for the diphenylacetylene. Other mononuclear platinum complexes also exhibit good catalytic activity for hydrosilylation catalysis of butadiynes [21].

The combination of evidence, strongly suggests that the catalytic activity exhibited by the mixed-metal cluster complexes reported here is produced principally by fragmentation products which are almost certainly mononuclear platinum complexes.

4. Supplementary material

Crystallographic data for the structural analysis have been deposited with the Cambridge Crystallographic Data Centre, CCDC nos. 139516 for **1**, 139517 for **2**, 139518 for **3**, 139519 for **4**, 139520 for **5**, 139521 for **6**. Copies of this information may be obtained free of charge from The Director, CCDC, 12 Union Road, Cambridge CB2 1EZ, UK (Fax: +44-1223-336-033; e-mail: deposit@ccdc.cam.ac.uk or www: http://www.ccdc.cam.ac.uk).

Acknowledgements

This research was supported by the Division of Chemical Sciences of the Office of Basic Energy Sciences of the U.S. Department of Energy.

References

[1] (a) J.H. Sinfelt, Bimetallic Catalysts. Discoveries, Concepts and Applications; Wiley, New York, 1983. (b) J.H. Sinfelt, Adv. Chem. Eng. 5 (1964) 37. (c) J.H. Sinfelt, Sci. Am. 253 (1985) 90. (d) J.H. Sinfelt, Acc. Chem. Res. 10 (1977) 15. (e) W.M.H.J. Sachtler, Mol. Catal. 24 (1984) 1. (f) L.J. Guczi, Mol. Catal. 25 (1984) 13. (g) W.M.H. Sachtler, R.A. van Santen, Adv. Catal. 26 (1977) 69. (h) Ponec, Adv. Catal. 32 (1983) 149. (i) J. Biswas, G.M. Bickle, P.G. Gray, D.D. Do, J. Barbier, Catal. Rev. Sci. Eng. 30 (1988) 30, 161. (j) G. Diaz, F. Garin, G. Maire, J. Catal. 82 (1983) 13. (k) D.W. Goodman, J.E. Houston, Science 236 (1987) 403. (l) J.A. Rodriguez, Surf. Sci. Rep. 24 (1996) 223. (m) B. Früberger, J.G.J. Chen, Catal. Lett. 45 (1997) 85.

[2] (a) W.M.H. Sachtler, What makes a Catalyst Selective?, Faraday Disc. Chem. Soc. 72 (1981) 7. (b) W.M.H. Sachtler, J. Mol. Catal. 25 (1984) 1. (b) L. Guczi, J. Mol. Catal. 25 (1984) 13. (c) W.M.H. Sachtler, R.A. van Santen, Adv. Catal. 26 (1977) 69.

[3] (a) D.W. Goodman, J.E. Houston, Science 236 (1987) 403. (b) M. Ichikawa, Adv. Catal. 38 (1992) 283.

[4] (a) P.R. Raithby, Platinum Metals Rev. 42 (1998) 146. (b) E.L. Muetterties, Bull. Soc. Chim. Belg. 85 (1976) 451. (c) E.L. Muetterties, Bull. Soc. Chim. Belg. 84 (1975) 959.

[5] (a) E.L. Muetterties, T.N. Rhodin, E. Band, C.F. Bruker, W.R. Pretzer, Chem Rev. 79 (1979) 91. (b) B.C. Wiegand, C.M. Friend, Chem. Rev. 92 (1992) 491. (c) R.J. Puddephatt, L. Manojlovic-Muir, K.W. Muir, Polyhedron 9 (1990) 2767.

[6] R.D. Adams, T.S. Barnard, Organometallics 17 (1998) 2885.

[7] H.S. Hilal, S. Khalaf, W. Jondi, J. Organomet. Chem. 452 (1993) 167.

[8] D.M. Blake, D.M. Roundhill, Inorg. Syn. 18 (1978) 12.

[9] P. Rushman, G.N. van Buuren, M. Shiralian, R.K. Pomeroy, Organometallics 2 (1982) 693.

[10] B.F.G. Johnson, J. Lewis, B.E. Reichert, K.T. Schorpp, G.M.J. Sheldrick, Chem. Soc. Dalton Trans. (1977) 1417.

[11] E.J. Forbes, N. Goodhand, D.L. Jones, T.A. Hamor, J. Organomet. Chem. 182 (1979) 143.

[12] M.I. Bruce, J.M. Guss, R. Mason, B.W. Skelton, A.H. White, J. Organomet. Chem. 251 (1983) 261.

[13] M.V. Capparelli, Y. De Sanctis, A.J. Arce, Acta. Crystallogr. C51 (1995) 1819.

[14] M.I. Bruce, M.J. Liddell, C.A. Hughes, B.W. Skelton, A.H. White, J. Organomet. Chem. 347 (1988) 181.

[15] F. Piacenti, M. Bianchi, P. Frediani, E. Beneditti, Inorg. Chem. 10 (1971) 2759.

[16] A.U. Harkonen, M. Ahlgren, T.A. Pakkanen, J. Pursiainen, J. Organomet. Chem. 530 (1997) 191.

[17] International Tables for X-ray Crystallography, vol. IV, Kynoch Press, Birmingham, UK, 1975, table 2.2B, pp. 99–101.

[18] International Tables for X-ray Crystallography, vol. IV, Kynoch Press, Birmingham, UK, 1975, table 2.3.1, pp. 149–150.

[19] (a) M. Brockmann, H. Dieck, J. Klauss, J. Organomet. Chem. 301 (1986) 209. (b) M. Green, J.L. Spencer, F.G.A. Stone, C.A. Tsipis, J. Chem. Soc. Dalton Trans. (1977) 1525.

[20] T. Kusumoto, K. Ando, T. Hiyama, Bull. Chem. Soc. Jpn. 65 (1992) 1280.

[21] S. Yamazaki, A.J. Deeming, D.M. Speel, Organometallics 17 (1998) 775.

[22] L.J. Farrugia, Adv. Organomet. Chem. 31 (1990) 301.

[23] (a) I. Ojima, R.J. Donovan, P. Ingallina, N. Clos, W.R. Shay, M. Eguchi, Q. Zeng, A. Korda, J. Cluster Sci. 3 (1992) 423. (b) I. Ojima, N. Clos, R.J. Donovan, P. Ingallina, Organometallics 9 (1990) 3127.